State-selected studies of the electron capture by Ne^{3+} and Ne^{4+} ions from N_2 and O_2 molecules

E. Y. Kamber and S. M. Ferguson
Department of Physics, Western Michigan University, Kalamazoo, Michigan 49008-5151
(Received 13 July 1999; revised manuscript received 24 July 2000; published 5 January 2001)

State-selective differential cross sections for single-electron capture processes in collisions of Ne^{q+} ($q=3$ and 4) ions with N_2 and O_2 have been studied experimentally at laboratory impact energies between 75 and 600 eV and scattering angles between 0° and 8° by means of a translational energy-gain spectroscopy technique. For the N_2 target, zero-angle translational energy spectra show that the capture occurs mainly into $3s$ and $3d$ states of the projectile product $Ne^{(q-1)+}$, respectively, for the ion charge states $q=3$ and 4. For the O_2 target, the dominant reaction channels are due to capture into $3p$ and $3d'$, respectively, for charge states $q=3$ and 4. In collisions of Ne^{3+} with N_2 and O_2, contributions from processes commencing with a long-lived metastable state $Ne^{3+}(2p^3\ ^2D)$ are detected. Other channels due to capture accompanied by target excitation are found to open at large scattering angles. The angle and energy dependence of cross sections for single-electron capture by Ne^{q+} ($q=3$ and 4) ions from N_2 and O_2 are also measured.

DOI: 10.1103/PhysRevA.63.022701 PACS number(s): 34.70.+e, 82.30.Fi

I. INTRODUCTION

The study of single-electron capture in very slow collisions of multiply charged ions with molecular targets has recently received considerable theoretical and experimental attention. Such processes are of importance in applications to the studies of low- to high-temperature astrophysical plasmas and properties of the earth's atmosphere. They are also relevant to diagnostics of plasma parameters, plasma heating, and modeling of the comparatively cool edge of the fusion plasma, where effective control and removal of impurities is of crucial importance.

Translational energy spectroscopy has been extensively used to study state-selective single-electron capture by multiply charged neon ions from rare-gas atoms and atomic and molecular hydrogen. However, in the case of N_2 and O_2 targets, there have been no previous experimental measurements of cross sections, differential in translational energy gain and projectile scattering angle, for state-selective single-electron capture at low energies, to our knowledge.

In our previous work we used a differential energy-gain spectrometer [1,2], capable of measuring simultaneously the scattering angle and the energy gain of projectile products in ion-atom collisions, for the study of state-selective single-electron capture from atomic targets by Ar^{q+} ($q=4-6$) and Ne^{q+} ($q=3-5$) ions at laboratory impact energies between 150 and 600 eV. In the work reported here we have extended our measurements to molecular targets. Briefly, multiply charged neon ions were produced in a recoil ion source by using 25 MeV F^{4+} ions from the Western Michigan University tandem Van de Graaff accelerator as a pump beam. An einzel lens was used to focus the ion beam extracted from the source into a 180° double-focusing magnet. After momentum selection, the ion beam was again focused by two pairs of deflectors and directed into a gas cell containing low-pressure target gas to ensure single-collision conditions. Ions scattered through a nominal angle θ into a solid angle ($\Delta\Omega$) of about 3×10^{-3} sr were energy analyzed by means of a 90° double-focusing electrostatic analyzer (ESA), and then detected by a one-dimensional position sensitive channel-plate detector located at the focal plane of the ESA. The scattering angle θ is selected by means of an aperture (1 mm diameter) in front of the ESA.

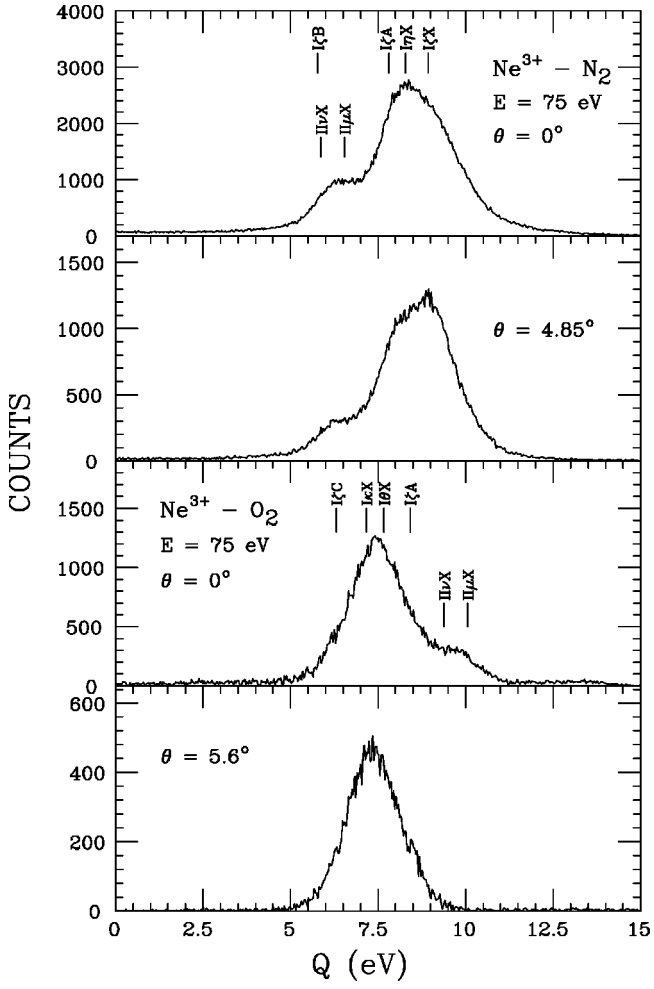

FIG. 1. Translational energy-gain spectra for single-electron capture by 75 eV Ne^{3+} ions from N_2 and O_2 at different projectile laboratory scattering angles.

TABLE I. Single-electron capture reaction channels for collisions of Ne^{3+} ions with N_2 and O_2.

Reactants and initial states	Product final states	ΔE (ev)	Designation of reaction process
Ne^{3+} $(2p^3\ ^4S)+N_2(X\ ^1\Sigma_g^+)$	Ne^{2+} $(3s\ ^5S)+N_2^+(X\ ^2\Sigma_g^+)$	8.93	IζX
	Ne^{2+} $(3s\ ^3S)+N_2^+(X\ ^2\Sigma_g^+)$	8.28	IηX
	Ne^{2+} $(3s\ ^5S)+N_2^+(A\ ^2\Pi_u)$	7.81	IζA
	Ne^{2+} $(3s\ ^5S)+N_2^+(B\ ^2\Sigma_u)$	5.77	IζB
Ne^{3+} $(2p^{3\,2}D)+N_2$ $(X\ ^1\Sigma_g^+)$	Ne^{2+} $(2p^3(^2P)3s\ ^3P)+N_2^+(X\ ^2\Sigma_g^+)$	6.54	IIμX
	Ne^{2+} $(2p^3(^2P)3s\ ^1p)+N_2^+(X\ ^2\Sigma_g^+)$	5.87	IIνX
Ne^{3+} $(2p^3\ ^4S)+O_2(X\ ^3\Sigma_g^-)$	Ne^{2+} $(3p\ ^5P)+O_2^+(X\ ^2\Pi_g)$	7.67	IθX
	Ne^{2+} $(3p\ ^3P)+O_2^+(X\ ^2\Pi_g)$	7.16	IκX
	Ne^{2+} $(3s\ ^5S)+O_2^+(a\ ^4\Pi_u)$	8.41	IζA
	Ne^{2+} $(3s\ ^5S)+O_2^+(b\ ^4\Sigma_g^-)$	6.3	IζC
Ne^{3+} $(2p^3\ ^2D)+O_2(X\ ^3\Sigma_g^-)$	Ne^{2+} $(2p^3(^2P)3s\ ^3P)+O_2^+(X\ ^2\Pi_g)$	9.95	IIμX
	Ne^{2+} $(2p^3(^2P)3s\ ^1p)+O_2^+(X\ ^2\Pi_g)$	9.28	IIνX

II. RESULTS AND DISCUSSION

In the process of single-electron capture by multiply charged ions from atomic or molecular targets, the projectile gains an amount of energy (Q) that depends on the participating electronic states, masses of the projectile and target, and scattering angle of the projectile ions. In a classical two-body collision, the translational energy of an ion undergoing inelastic scattering differs from the impact energy of the projectile ion E_0 by

$$Q=E-E_0=\Delta E-\Delta K, \tag{1}$$

where ΔE is the energy defect of the reaction, and ΔK is the translational energy given to the target and is given by

$$\Delta K=\frac{m_P}{m_P+M}(1-\cos\theta_P)\left[\frac{2ME_0}{m_P+M}-\Delta E\right]+\left[\frac{m_P(\Delta E)^2}{4ME_0}\right]\cos\theta_P, \tag{2}$$

where m_P and M are, respectively, the projectile and target masses, and θ_P is the final laboratory scattering angle of the projectile [3]. However, for these collision systems values of ΔK calculated on the basis of zero and nonzero scattering angles are found to be small. This indicates that we can assume that $Q=\Delta E$. In the present measurements, the translational energy spectra are expressed in terms of the Q values and no correction (i.e., ΔK) was added to the measured energy gain.

The energy levels used in calculating the energy defect (ΔE) were taken from Moore [4], Bashkin and Stoner [5], and other sources [6,7]. The product states are identified by the energy gain Q, measured from the translational energy-gain spectra obtained with a differential energy-gain spectrometer. The energies (ΔE) were calculated assuming that the molecular targets and their product ions were at the lowest vibrational levels ($\nu=0$). The observed reaction channels are labeled according to the notation previously used by Kamber *et al.* [8]. The designations I and II represent the ground and first metastable states of the incident ion, respectively, while $\alpha,\beta,\gamma,\ldots$ represent the ground and successive higher excited states of the projectile product; $X,A,B,\ldots$ represent the ground and higher excited states of the target product. To identify the reaction channels involved, the energy-gain spectra for Ne^{3+}-Ar and Ne^{4+}-Ar collision systems [2] were used as a standard to calibrate the Q scale for the $Ne^{3+,4+}$-N_2 and -O_2 systems. In the latter collision systems, single-electron capture spectra are observed to be broader. This is probably due to the vibrational states of the target products N_2^+ and O_2^+, which are smaller than the present energy resolution of 1.1 eV. The spectra were normalized to the same target densities and total amount of pump beam charge collected at the Faraday cup after it passed through the interaction region in the recoil-ion source.

In the following sections the results for single-electron capture processes in collisions of Ne^{q+} ions ($q=3$ and 4) with N_2 and O_2 are presented and discussed. The data are classified according to the translational energy-gain spectra, differential cross sections, and energy dependence total cross sections measurements.

A. Translational energy-gain spectra

1. Ne^{3+} collisions with N_2 and O_2

Figure 1 shows the translational energy-gain spectra for the formation of Ne^{2+} ions from the reaction of 75 eV Ne^{3+} ions with N_2 and O_2 at different projectile laboratory scattering angles. The possible exit channels following single-electron capture are listed in Table I.

In Ne^{3+}-N_2 collisions, the observed collision spectrum at 0° scattering angle is dominated by a peak due to capture from the ground state $Ne^{3+}(2p^3\ ^4S)$ ions into the $3s\ ^{5,3}S$ excited states of the Ne^{2+} product ions with production of N_2^+ in the ground state ($X\ ^2\Sigma_g^+$) via reaction channels IζX and IηX. Contributions from capture accompanied by the

excitation of the target product via the reaction channel IζA cannot be ruled out.

The broad peak, centered around $Q=6.5$ eV, is due to capture from the metastable state $2p^3\ ^2D$ of Ne^{3+} into the $2p^3(^2P)3s$ states of Ne^{2+} via IIμX and IIνX channels. There can also be contributions due to transfer excitation via the reaction channel IζB.

At a scattering angle of 4.85°, single-electron capture into the $3s$ state of Ne^{3+} remains dominant, but the relative importance of the reaction channels correlated with the presence of the metastable state $2p^3\ ^2D$ in the Ne^{3+} ion beam decreases. This indicates that the angular distribution for capture into the $3s$ state is peaked in the forward direction in Ne^{3+}-N_2 collisions.

In Ne^{3+}-O_2 collisions, the dominant peak at 0° scattering angle corresponds to capture from ground state incident $Ne^{3+}(2p^3\ ^4S)$ into the $3p\ ^{5,3}P$ states of Ne^{2+} with production of $O_2{}^+$ in the ground state ($X\ ^2\Pi_g$) via IθX and IκX channels, with contribution from the transfer excitation channel IζA. The structure (IζC) on the lower-energy side of the dominant peak corresponds to capture into $3s\ ^5S$ states with target excitation to the ($b\ ^4\Sigma_g$) state of $O_2{}^+$. The smaller peak at about 10 eV correlates with capture from the metastable state $2p^3\ ^2D$ of Ne^{3+} into the $2p^3(^2P)3s$ states of Ne^{2+} via IIμX and IIνX channels. As the angle is increased, capture into the $3p$ states of Ne^{2+} remains dominant, whereas the relative importance of the reaction channels IIμX and IIνX is strongly decreased, and the small peak completely disappears for scattering angles $\theta \geqslant 5.6°$.

2. Ne^{4+} collisions with N_2 and O_2

Figure 2 shows the translational energy-gain spectra for single-electron capture by 100 eV Ne^{4+} ions from N_2 and O_2 at different projectile laboratory scattering angles, and the possible reaction channels following single-electron capture are listed in Table II. For the Ne^{4+}-N_2 system, the zero-degree spectrum shows only one peak; this peak correlates with single-electron capture into the $3d$ excited state of Ne^{3+} from the ground state Ne^{4+} ($2p^2\ ^3P$) ion with production of $N_2{}^+$ in the ground state ($X\ ^2\Sigma_g^+$) via the reaction channels IπX. There is also some contribution from an unresolved reaction at about 11.5 eV, involving transfer excitation into the $2p^2(^1D)3p\ ^2F$ state of Ne^{3+} accompanied by excitation of the target product into the excited state ($A\ ^2\Pi_u$) of $N_2{}^+$ (channel IoA).

At the scattering angle of 7.83°, single-electron capture into the $3d$ state remains dominant, but the relative importance of capture into the $2p^2(^1S)3s$ and $3p$ states gradually increases. This indicates that the angular distribution for capture into $3d$ is more strongly peaked in the forward direction than for the process associated with capture into $2p^2(^1S)3s$ and $3p$ states.

For the Ne^{4+}-O_2 collisions, the observed spectrum at 0° scattering angle is dominated by reaction channel IσX with unresolved contributions from the transfer excitation IπA channel. The peak at around 6.5 eV is due to the reaction channel IνX, while the long tail located at $Q \geqslant 12$ eV is due

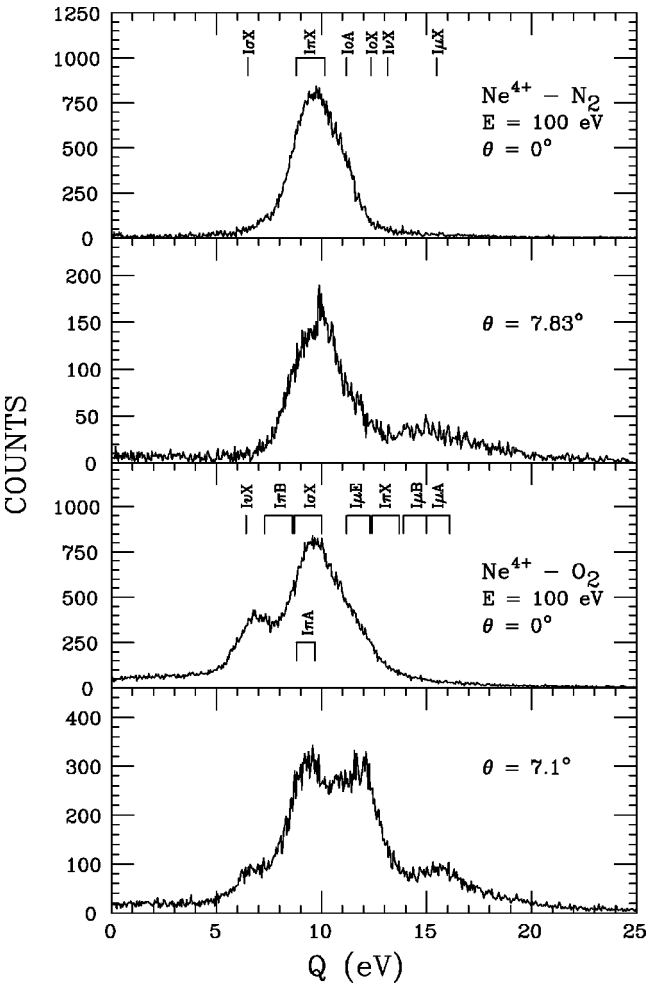

FIG. 2. Translational energy-gain spectra for single-electron capture by 100 eV Ne^{4+} ions from N_2 and O_2 at different projectile laboratory scattering angles.

to capture into the $3p$ state of Ne^{3+} with the production of $O_2{}^+$ in the excited states a $^4\Pi_u$, $A\ ^2\Pi_u$, and $D\ ^2\Sigma_g$ (IμA, IμB, . . . channels) (see Fig. 2).

As the scattering angle increases, single-electron capture into the $2p^2(^1D)3d$ state of Ne^{3+} (IσX) remains dominant. However, the importance of capture into $3p$ accompanied by excitation of the target product (IμA and IμB channels) increases, and the relative importance of the reaction channel IνX decreases. In this collision system, we observed a particularly interesting feature of the scattering angle dependence of single-electron capture spectra. With increasing scattering angles, contributions from avoided crossings at smaller internuclear separations (large Q values) become gradually more important, as one would expect. In general, at forward scattering or smaller angles, the larger impact parameter collisions play an important role in the electron capture process since the avoided crossings at small internuclear separation cannot be reached and make no contribution. As the angle is increased, contributions from successively smaller internuclear separation regions make their appearance.

TABLE II. Single-electron capture reaction channels for collisions of Ne^{4+} ions with N_2 and O_2.

Reactants and initial states	Product and final states	ΔE (eV)	Designation of reaction process
Ne^{4+} $(2p^2\ ^3P)+N_2(X\ ^1\Sigma_g^+)$	Ne^{3+} $(3p\ ^4S)+N_2^+(X\ ^2\Sigma_g^+)$	15.5	$I\mu X$
	Ne^{3+} $(2p^2(^1S)3s\ ^2S)+N_2^+(X\ ^2\Sigma_g^+)$	13.2	$I\nu X$
	Ne^{3+} $(2p^2(^1D)3p\ ^2F)+N_2^+(X\ ^2\Sigma_g^+)$	12.6	IoX
	Ne^{3+} $(2p^2(^1D)3p\ ^2F)+N_2^+(A\ ^2\Pi_u)$	11.5	IoA
	Ne^{3+} $(3d)+N_2^+(X\ ^2\Sigma_g^+)$	8.8–10.2	$I\pi X$
	Ne^{3+} $(2p^2(^1D)3d\ ^2D)+N_2^+(X\ ^2\Sigma_g^+)$	6.5	$I\sigma X$
Ne^{4+} $(2p^2\ ^3P)+O_2(X\ ^3\Sigma_g^-)$	Ne^{3+} $(3p)+O_2^+(a\ ^4\Pi_u)$	15–16.1	$I\mu A$
	Ne^{3+} $(3p)+O_2^+(A\ ^2\Pi_u)$	14–15.1	$I\mu B$
	Ne^{3+} $(3d)+O_2^+(X\ ^2\Pi_g)$	12.3–13.6	$I\pi X$
	Ne^{3+} $(3p)+O_2^+(D\ ^2\Sigma_g)$	11.3–12.4	$I\mu E$
	Ne^{3+} $(2p^2(^1D)3d)+O_2^+(X\ ^2\Pi_g)$	8.8–10	$I\sigma X$
	Ne^{3+} $(3d)+O_2^+(a\ ^4\Pi_u)$	8.6–9.6	$I\pi A$
	Ne^{3+} $(3d)+O_2^+(A\ ^2\Pi_u)$	7.3–8.6	$I\pi B$
	Ne^{3+} $(4s\ ^4P)+O_2^+(X\ ^2\Pi_g)$	6.5	$I\nu X$

B. Differential cross sections

The experimental total differential cross sections $(d\sigma/d\Omega)$ for single-electron capture by Ne^{q+} ions from N_2 and O_2 for $q=3$ and 4 are shown in Fig. 3. The dashed curves in Fig. 3 are to guide the eye. The differential cross sections were found using the translational energy-gain technique, by calculating the area under the peaks (total intensity) in the energy-gain spectra at different projectile laboratory scattering angles. The general features of the distributions are qualitatively explained in terms of a semiclassical model based on Coulomb potential curves [9]. The traditional two-state model has been used to estimate the critical angle θ_c, which corresponds to capture at an impact parameter equal to the crossing radius, by assuming that capture occurs at a localized curve crossing between the potential energy curves for entrance and exit channels. For small laboratory scattering angles, $\theta_c=Q/2E_0$, where Q is the exoergicity of the collision and E_0 is the laboratory impact energy. The calculations of differential cross sections usually show a minimum at θ_c. This angle separates the events scattered at smaller angles due to capture on the way out and events scattered at larger angles due to capture on the way into the collision.

For 75 eV Ne^{3+}-N_2 collisions (see Fig. 3), the distribution maximizes near the critical angle $\theta_c=3.3°$, which corresponds to the $3s\ ^3S$ capture channel at an impact parameter equal to the crossing radius. The forward peak clearly represents the contribution from capture into the final channel on the way out from the collision.

For 75 eV Ne^{3+}-O_2 collisions, the distribution increases below $\theta_c=2.9°$ for capture into the $3p$ state of the Ne^{2+} ion, with a significant peak located near 3.8° (see Fig. 3). The structure below θ_c represents contributions from capture on the way out from the collision with a valley located near $\theta=1.5°$, which is a rainbow effect caused by $4s$ promotion of the entrance channel. The peak occurring at larger angles (i.e., $\theta\geqslant 2.9°$) is almost entirely contributions from capture that take place on the way into the collision, i.e., the upper branch of the deflection function.

For 100 eV Ne^{4+}-N_2 collisions, the data show that the distribution for capture into the $3d$ state is peaked in the forward direction and is a relatively smooth function. For 100 eV Ne^{4+}-O_2 collisions (see Fig. 3), the measurements show that the projectile products are distributed forward inside the critical angle $\theta_c=2.7°$, indicating that capture took place on the way out of the collision.

C. Total cross sections

The measured total cross sections for single-electron capture by Ne^{q+} ions ($q=3$ and 4) from N_2 and O_2 at laboratory collision energies between 25 and 150 qeV are shown in Fig. 4. For these measurements, an angular acceptance of about $\mp 10°$ was used after removing the angular selector in front of the ESA. The absolute scales for the cross sections were evaluated by normalizing to the total amount of fast beam charge collected and by using the total single-electron capture cross section measurements of Justiniano *et al.* [10] for Ne^{q+}-He collisions.

For Ne^{3+} ions, the total cross sections oscillate with increasing collision energy about averages values of 40 and 60×10^{-16} cm^2, respectively, for O_2 and N_2 targets, a behavior that is well documented for such collisions at low energies. This is attributed to the availability of many capture channels, which are situated nearly at the center of the reaction window. For Ne^{4+} ions, the total cross sections slowly increase with the collision energy. This can also be understood from the reaction window, which gets broader with increasing energy, and therefore capture channels with large Q values get an increasing probability.

III. CONCLUSION

Doubly differential cross sections, in energy and angle, for single-electron capture by very low-energy Ne^{q+} ions

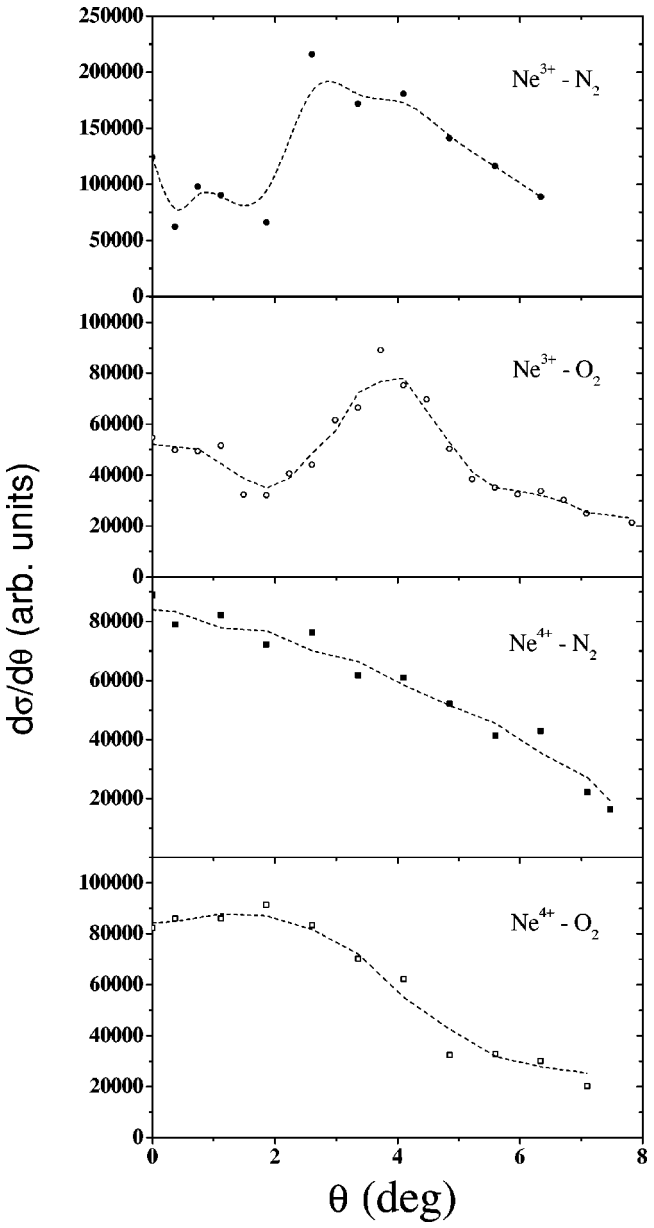

FIG. 3. Experimental differential cross sections ($d\sigma/d\Omega$) for single-electron capture by 75 eV Ne^{3+} and 100 eV Ne^{4+} ions from N_2 and O_2. Smooth lines are drawn to guide the eye.

($q=3$ and 4) from N_2 and O_2 have been studied by means of translational energy-gain spectroscopy. In addition to pure single-electron capture channels, we also detected weaker channels due to transfer excitation (i.e., capture accompanied by target excitation) and the presence of the metastable state $Ne^3(2p^3\,{}^2D)$ in the primary ion beam. In these collision systems, no clear evidence of molecular dissociation was observed. We have also studied differential cross sections for single-electron capture processes in the collision systems mentioned. For Ne^{3+}-N_2 and -O_2 collisions, the angular distribution spectra contain a main peak lying just inside a critical angle θ_c, corresponding to capture at an impact parameter equal to the crossing radius of the dominant reaction channel. The peaks are qualitatively explained by a two-state model and are attributed to a capture process on the way out from the collision. For collisions of Ne^{4+} with N_2 and O_2, the mean peaks of the distributions lie at angles greater than θ_c, which represent contributions from capture that takes place on the way into the collision. The energy dependence of cross sections for single-electron capture by Ne^{q+} ions ($q=3$ and 4) from N_2 and O_2 were also measured. No data on state-selective single-electron capture by low-energy Ne^{q+} ions from N_2 and O_2 are, however, available for comparison.

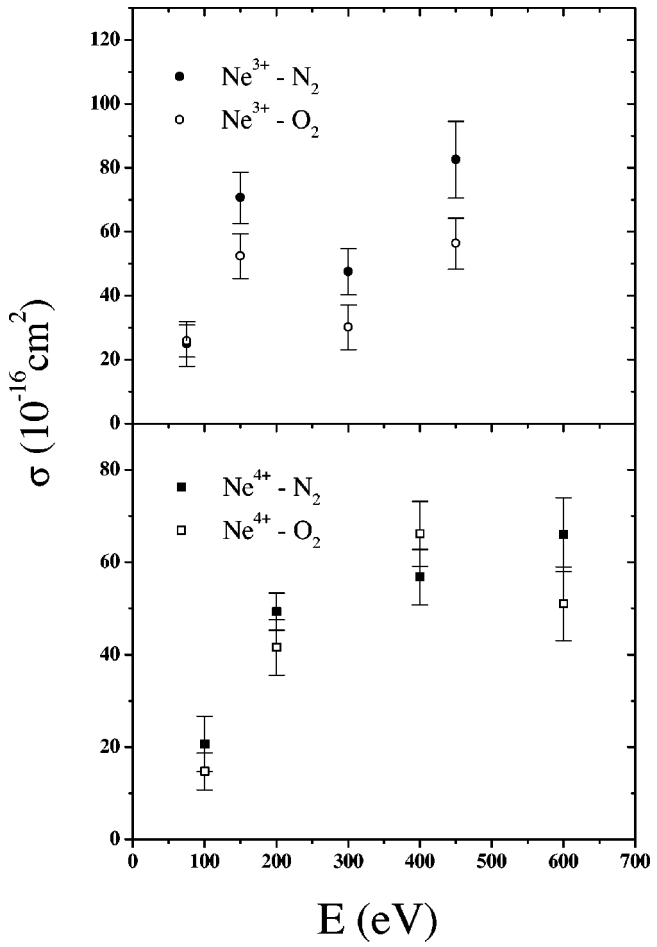

FIG. 4. Total cross sections for single-electron capture by Ne^{q+} ions ($q=3$ and 4) from N_2 and O_2.

[1] S. Yaltkaya, E. Y. Kamber, and S. M. Ferguson, Phys. Rev. A **48**, 382 (1993).

[2] R. Said, E. Y. Kamber, S. Yaltkaya, and S. M. Ferguson, J. Phys. B **27**, 3993 (1994).

[3] *Collision Spectroscopy*, edited by R. G. Cooks (Plenum, New York, 1978), p. 252.

[4] C. E Moore, *Atomic Energy Levels*, Natl. Bur. Stand. (U.S.) Circ. No. 467 (U.S. GPO, Washington, DC, 1970).

[5] S. Bashkin and J. O. Stoner, Jr., *Atomic Energy Levels and Grotrian Diagrams* (North-Holland, Amsterdam, 1978).

[6] J. W. Robinson, *CRC Handbook of Spectroscopy* (CRC, Boca Raton, FL, 1974).

[7] R. D. Levin and S. G. Lias, *Ionization Potential and Appearance Potential Measurements 1971–1981*, Natl. Bur. Stand. Ref. Data Ser. Natl. Bur. Stand. (U.S.) Circ. No. 71 (U.S. GPO, Washington, DC, 1982).

[8] E. Y. Kamber, D. Mathur, and J. B. Hasted, J. Phys. B **15**, 263 (1982).

[9] L. R. Andersson, H. Donard, and A. Barany, Nucl. Instrum. Methods Phys. Res. B **23**, 54 (1987).

[10] E. Justiniano, C. L. Cocke, T. J. Gray, R. Dubois, C. Can, W. Waggoner, R. Schuch, H. Schmidt-Böcking, and H. Ingwersen, Phys. Rev. A **29**, 1088 (1984).